Journal of Molecular Catalysis A: Chemical 425 (2016) 266–274

Contents lists available at ScienceDirect

Journal of Molecular Catalysis A: Chemical

journal homepage: www.elsevier.com/locate/molcata

Valorization of biomass derivatives: Keggin heteropolyacids supported on titania as catalysts in the suitable synthesis of 2-phenoxyethyl-2-furoate

Angélica M. Escobar Caicedo[a], Julián A. Rengifo-Herrera[a,*], Pierre Florian[c], Mirta N. Blanco[a], Gustavo P. Romanelli[a,b,**], Luis R. Pizzio[a]

[a] Centro de Investigación y Desarrollo en Ciencias Aplicadas "Dr. J.J. Ronco" (CINDECA), Departamento de Química, Facultad de Ciencias Exactas, UNLP-CCT La Plata, CONICET, 47 No. 257, 1900 La Plata, Buenos Aires, Argentina
[b] Cátedra de Química Orgánica, CISAV, Facultad de Ciencias Agrarias y Forestales, UNLP, Argentina
[c] CNRS, CEMHTI UPR3079, Université d'Orléans, F-45071 Orléans, France

ARTICLE INFO

Article history:
Received 11 August 2016
Received in revised form 14 October 2016
Accepted 19 October 2016
Available online 19 October 2016

Keywords:
Heteropolyacids
TiO_2
Esterification
2-Phenoxyethyl-2-furoate
Solvent-free reaction

ABSTRACT

Titania modified by tungstophosphoric (TPA) and tungstosilicic (TSA) acid (30% w/w) were synthesized by the sol-gel method, using urea as low cost pore-forming agent and annealing at 500 °C for 2 h (TiO_2/TPA and TiO_2/TSA respectively). The obtained materials were characterized by ^{31}P, ^{29}Si, ^{1}H nuclear magnetic resonance (^{31}P, ^{29}Si, ^{1}H MAS-NMR), X-ray diffraction (XRD), X-ray photo-electron spectroscopy (XPS), Raman spectroscopy (FT-Raman), acid strength by potentiometric titration with *n*-butylamine. Mesoporous materials were obtained, without important microporosity, as determined from N_2 adsorption-desorption isotherms by the Brunauer-Emmett-Teller (BET) method. The XRD patterns of the modified samples exhibited only peaks of anatase phase. According $^{31}P/^{29}Si$ MAS-NMR and XPS studies, the main species present in the TiO_2/TPA and TiO_2/TSA samples are the Keggin anions by forming surface acid species, and probably surface complex between Keggin anion and titania as well. Solids were evaluated in the synthesis of 2-phenoxyethyl-2-furoate, by esterification of 2-furoic acid, a valuable product which can be obtained from biomass, with 2-phenoxyethanol, where TiO_2/TPA sample showed the highest catalytic activity. The reaction temperature, molar ratio acid:alcohol and catalyst amount were studied as variables using TiO_2/TPA sample. Results of catalytic activity and diffuse reflectance infrared Fourier transform spectroscopy (DRIFT-FT-IR) measurements suggested that the reaction mechanism may involve a protonated intermediate of 2-furoic acid polarizing the C=O bond of the acid, and leaving that can be easily attacked by 2-phenoxyethanol.

1. Introduction

High Brönsted acidity, thermal stability, low volatility, fast and reversible redox multielectronic transformations in mild conditions, lead to the heteropolyacids (HPAs), such as tungstophosphoric (TPA) and tungstosilicic (TSA) acids, suitable features as catalysts participating in different organic reactions [1,2]. However, these compounds present two important drawbacks to overcome: (i) their low surface area and (ii) the solubility in polar media, which limit their use as heterogeneous catalysts [2]. In order to overcome these problems, the HPAs have been supported on different substrates such as silica, titania, activated carbon, zirconia among others [3–8].

On the other hand, the esterification is one of the most important reactions in drug synthesis and the organic esters are important products and/or intermediates in the industrial production of fragrances, flavorings, polymers, polyesters, plasticizers, fatty acids, biofuels and paints [9]. For these reasons, the searching of novel, clean and sustainable methodologies for esters synthesis is a very important issue [10]. Solvent-free reactions have advantages as pollution reduction by organic solvents, and low costs due to the less use of reactive and process simplification by decreasing steps,

* Corresponding author.
** Corresponding author at: Centro de Investigación y Desarrollo en Ciencias Aplicadas "Dr. J.J. Ronco" (CINDECA), Departamento de Química, Facultad de Ciencias Exactas, UNLP-CCT La Plata, CONICET, 47 No. 257, 1900 La Plata, Buenos Aires, Argentina.
E-mail addresses: julianregifo@quimica.unlp.edu.ar (J.A. Rengifo-Herrera), gpr@quimica.unlp.edu.ar (G.P. Romanelli).

http://dx.doi.org/10.1016/j.molcata.2016.10.024
1381-1169/

such as removal of the solvent, which are important factors in the industry [11]. Esters are often synthesized by condensation reactions between carboxylic acids and alcohols using sulfuric acid, *p*-toluenesulfonic acid or phosphoric acid, all toxic and corrosive acids [12].

The esterification of several acids such as formic [13], oleic [14], acetic acid [6] using supported tungstophosphoric acid on zirconia and silica has already been reported on the literature, where capital parameters such as acid:alcohol ratio, catalyst amount, reaction temperature and catalyst recycle have been highlighted.

Furoic acid is a promising product in biomass valorization since it can be used as intermediate in pharmaceutical, food, cosmetics and perfumery industries [15]. This acid is produced from lignocellulosic material which comes from agricultural or forestry wastes [16].

In a previous study recently reported by some of us, TPA supported on zirconia was used as catalyst in esterification of 2-furoic acid with different alcohols [17]. Esterification reaction of 2-fuoric acid with 2-phenoxyethanol in the presence of TPA-zirconia catalysts led to the formation of 2-phenoxyethyl-2-furoate (estimated by GC–MS) and it was also found that parameters such as 2-fuoric acid:alcohol molar ratio and reaction temperature played an important role.

The aim of this study was to synthesize and characterize by multitechniques two catalysts based on tungstophosphoric and tungstosilicic acid supported on titania, studying the stability of immobilized TPA and TSA by XPS, $^{31}P/^{29}Si$ MAS NMR, FT-Raman. On the other hand, the acidity and the presence of acid sites were studied by potentiometric titration and ^{1}H MAS-NMR, respectively. Furthermore, it was evaluated their catalytic activity in the esterification of 2-furoic acid with 2-phenoxyethanol, taking into account variables such as temperature, acid-alcohol ratio and catalyst amount. Finally, the product 2-phenoxyethyl-2-furoate was analyzed by ^{1}H and ^{13}C NMR in order to confirm its presence.

2. Experimental section

2.1. Materials

The chemical substances used to synthesize the TiO_2-based samples and photocatalytic tests were: titanium tetraipropoxide (99% Sigma-Aldrich), urea (99% Sigma-Aldrich), tungstophosphoric acid ($H_3PW_{12}O_{40}{\cdot}23H_2O$) and tungstosilicic acid ($H_4SiW_{12}O_{40}{\cdot}23H_2O$) (99% Fluka), furoic acid (99% Sigma-Aldrich), 2-phenoxyethanol (99% Fluka), ethanol (Merck grade absolute), HCl (37% Carlo Erba). All chemicals were used as received.

2.2. Samples preparation

Titanium isopropoxide (26.7 g) was mixed with absolute ethanol (186.6 g) and stirred for 10 min to obtain a homogeneous solution under N_2 at room temperature, then 0.33 mL of 0.28 M HCl aqueous solution was dropped slowly into the above mixture to catalyze the sol–gel reaction and was left for 3 h. Then 120 g of urea–alcohol–water (1:5:1 wt ratio) solution was added to the hydrolyzed solution under vigorous stirring, to act as template, together with an ethanol solution of $H_3PW_{12}O_{40}{\cdot}23H_2O$ (TPA) or $H_4SiW_{12}O_{40}{\cdot}23H_2O$ (TSA). The amount of TPA or TSA solutions was fixed in order to obtain a concentration of 30% TPA or TSA (w/w).

The xerogels were dried at room temperature in a beaker. The solids were ground into powder and extracted with distilled water for three periods of 24 h to remove urea, in a system with continuous stirring. Finally, the solids were thermally treated at 500 °C for 2 h. The samples will be named TiO_2-TPA and TiO_2-TSA, respectively.

The TPA and TSA content on the TiO_2/TPA and TiO_2/TSA samples were estimated as the difference between the W amount contained in the heteropolyacid solution originally used for the impregnation and the amount of W in the water solutions obtained after the solid washing (in order to remove the urea). The W content was determined by atomic absorption spectrometry using a Varian AA Model 240 spectro-photometer as it was already reported in a previous study [18]. The calibration curve method was used with standards prepared in the laboratory. The analyses were carried out at a wavelength of 254.9 nm, bandwidth 0.3 nm, lamp current 15 mA, phototube amplification 800 V, burner height 4 mm, and acetylene–nitrous oxide flame (11:14).

2.3. Samples characterization

2.3.1. Nuclear magnetic resonance spectroscopy (NMR)

^{29}Si and ^{31}P MAS-NMR experiments were performed on a 9.4 T Avance Bruker Spectrometer operating at 161.9 MHz and 79.5 MHz respectively. It was used a 4 mm diameter rotor spinning at 10 kHz and applied a Bloch decay (single pulse acquisition) with a radio-frequency field of 100 kHz (^{31}P) and 35 kHz (^{29}Si) and pulse width of 10°. Due to the very small amount of NMR active nuclei in the sample, no relaxation time measurement could be performed and it was chosen a recycle delay of 15 s (^{31}P) and 1s (^{29}Si) based on various trials while accumulating between 21120 (3.7 days) and 642600 (7.5 days) scans, respectively. ^{1}H MAS-NMR experiments were performed on a 17.6 T Avance III Bruker spectrometer operating at 750.3 MHz. Hahn echo experiments were performed spinning at 30 kHz to remove the large probe background using a delay of 5 rotor periods (160 μs) and a radio-frequency field strength of 100 kHz. ^{31}P spectra have been referenced to a 1 M solution of H_3PO_4, whereas ^{29}Si and ^{1}H ones have been referenced to tetramethylsilane.

2.3.2. Fourier transform raman spectroscopy (FT-Raman)

Raman scattering spectra were recorded on a Raman Horiba Jobin-Yvon T 64000 instrument with an Ar+ laser source of 488 nm wavelength in a macroscopic configuration.

2.3.3. Acid strength by potentiometric titration

The solid (0.05 g) was suspended in acetonitrile (Merck) and stirred for 3 h. Then, the suspension was titrated with 0.05 N n-butylamine (Carlo Erba) in acetonitrile using Metrohm 794 Basic Titrino apparatus with a double junction electrode.

2.3.4. Atomic absorption spectrometry (AAS)

Tungsten (W) determination was carried out using an atomic absorption spectrometer Varian AA model 240 spectrophotometer. Calibration method was used with in house prepared standards. Analysis were carried out at a wavelength of 254.9 nm, bandwidth 0.3 nm, lamp current 15 mA, phototube amplification 800 V, burner height 4 mm, and acetylene-nitrous (11:4).

2.3.5. Diffuse reflectance fourier transform infrared spectroscopy (DRIFT-FTIR)

FTIR spectra were recorded on a FT-IR Perkin-Elmer Frontier instrument equipped with a DRIFT (Perkin Elmer) accessory. Spectra were recorded using 1024 scans having a resolution of 4 cm^{-1}.

2.3.6. X- ray photoelectron spectroscopy (XPS)

XPS analyses were carried out with XPS Analyzer Kratos model Axis Ultra with a monochromatic AlKα and charge neutralizer. The deconvolution software program was provided by Kratos, the manufacturer of the XPS instrument. All the binding energies were referred to the C1s peak at 285 eV of adventitious carbon. Powder

samples were prepared by deposition of the solid on carbon type stuck to the sample holder.

2.3.7. Textural properties

The specific surface area of the solids was determined from N_2 adsorption–desorption isotherms at liquid-nitrogen temperature. They were obtained using Micromeritics ASAP 2020 equipment. The samples were previously degassed at 100 °C for 2 h.

2.4. Catalytic activity

A glass flask (10 mL capacity) was used as reactor. Predetermined amounts of the reactants were charged into the flask and the temperature was raised to a prefixed value. Once the temperature was attained, the catalyst was added, and initial time sample was withdrawn. Samples were withdrawn from the organic phase at different times (0.5, 1, 3, 5, 7, 9 and 24 h). Each sample volume was 10 μL and was diluted with 100 μL of ethanol. The effect of different reaction temperatures, 2-furoic acid/2-phenoxyethanol molar ratio and catalyst amounts were studied. The blank experiment conditions were: 1 mmol 2-furoic acid, 10 mmol 2-phenoxyethanol, 125 °C, 24 h. The mixture was stirred at 700 rpm. The conversions were based on the limiting reactive determined by GC (Shimadzu, model 2014) using a FID detector and a capillary column (SPB-1, length 30 m, I.D. 32 mm, film thickness 1.00 μm) by calibration curve both the acid as the product. The product was confirmed by GC–MS analysis (Perkin Elmer Auto System/Q-Mass910) and ^{1}H NMR, ^{13}C NMR measurements (NMR Bruker Avance II-500 spectrometer).

2.4. Characterization of 2-phenoxyethyl-2-furoate

2-Phenoxyethyl-2-furoate mp: 66–68 °C (ethanol); ^{1}H NMR (500 MHz, $CDCl_3$): δ 4.31 (t, 2H, J = 7 Hz), 4.68 (t, 2H, J = 7 Hz), 6.53 (dd, 1H, J = 7.5 Hz, J = 7.5 Hz), 6.97 (m, 3H), 7.28 (m, 3H), 7.61 (dd, 1H, J = 7.5 Hz, J = 1.5 Hz), ^{13}C NMR (100 MHz, $CDCl_3$): δ 63.25, 65.80, 111.90,114.69, 118.43, 121.22, 129.53, 144.32, 146.55, 158.47,158.59. IEMS: m/z (I%): 232 (2) $M^{+\cdot}$, 139 (61), 95 (35), 77 (4), 51 (14), 44 (43), 39 (45), 32 (38), 28 (100).

2.5. Catalyst reuse

After the reaction, the catalyst was filtered, washed thoroughly with toluene, dried in a vacuum oven at room temperature and reused for the next reaction, following the procedure described above.

2.6. Adsorption of 2-furoic acid on catalyst

The adsorption of 2-furoic acid on the TiO_2/TPA catalyst was performed by adding 50 mg of TPA-TiO_2 catalyst to a mixture of 1 mmol of the acid and 1 mL of ethanol and stirring for 24 h is maintained. Then, the solid was dried in a vacuum oven at room temperature to remove the alcohol. Finally, the solid analyzed by DRIFT-FTIR.

3. Results and discussion

3.1. TiO_2, TiO_2-TPA and TiO_2-TSA characterization

The TPA and TSA content in the TiO_2/TPA and TiO_2/TSA samples was estimated as the difference between the W amount contained in the TPA or TSA solutions and the remaining amount of W in the solutions obtained during the washing of the xerogels. The results revealed that the W content (coming from TPA and TSA) in the samples was 22.6% (w/w) and 23.2% (w/w) for the TiO_2/TPA- and TiO_2/TSA samples, respectively, which agrees well with the initial W amount added as TPA and TSA during the synthesis (22.9% TPA (w/w) and 23.5% TSA (w/w) concentration).

Regarding the physical-chemical characterization, the MAS-NMR measurements of ^{31}P, ^{29}Si nuclei (Fig. 1a and b respectively) revealed that TiO_2/TPA and TiO_2/TSA samples exhibit the presence of Keggin anions of TPA and TSA. ^{31}P spectrum of bulk TPA (Fig. 1a.2) exhibited a doublet at −14.7 and −15 ppm, both signals are related to the presence of hydrated Keggin anion of tungstophosphoric acid [19,20]. On the other hand, the spectrum of TiO_2/TPA sam-

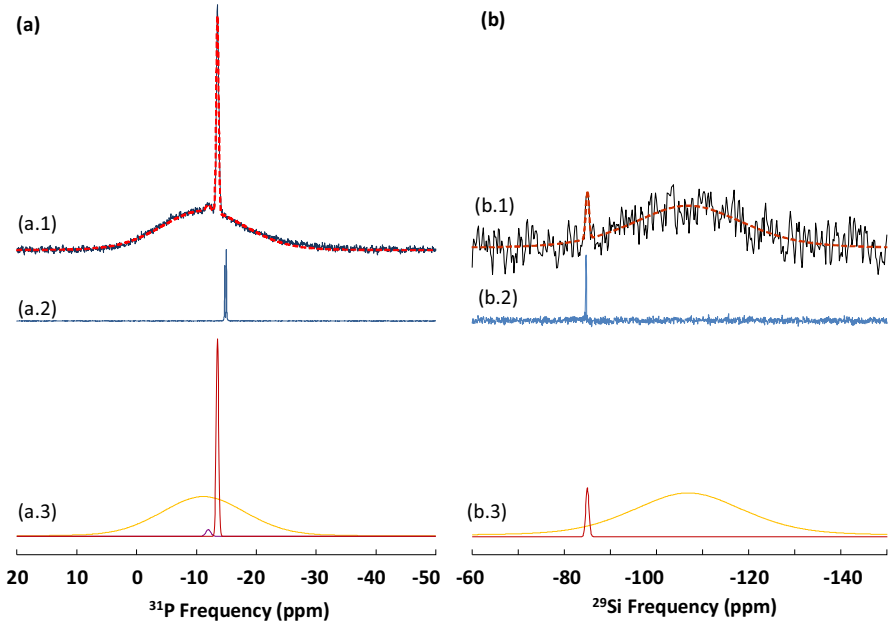

Fig. 1. (a) ^{31}P MAS-NMR spectra of (a.1) TiO_2-TPA and (a.2) TPA samples along with (a.3) the three individual components of the simulation displayed as a red line in (a.1). (b) ^{29} Si MAS-NMR spectra of (b.1) TiO_2-TSA and (b.2) TSA samples along with (b.3) the two individual components of the simulation displayed as a red line in (b.3). (For interpretation of the references to colour in this figure legend, the reader is referred to the web version of this article.)

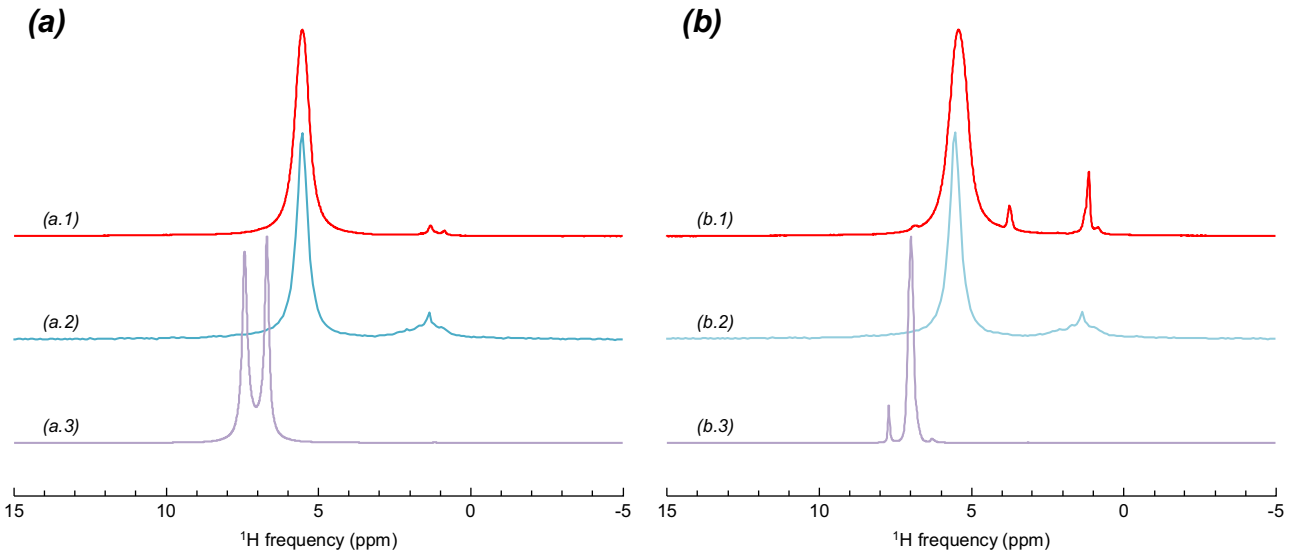

Fig. 2. ^{1}H MAS-NMR spectra of pristine TiO_2, (a.2, b.2) bulk TPA (a.3) and (b.3) bulk TSA, and TiO_2-TPA (a.1), and TiO_2-TSA (b.1) samples.

ple exhibited an intense signal at −13.5 ppm and also a broad peak ranging from 1 to −20 ppm (Fig. 1a.1). According to the deconvolution, the latter wide signal (Fig. 1a.3) presented a maximum at −12 ppm, and it was absent from the "blank" experiment performed on the pure TiO_2 precursor. Signals at −13.5, −11.2 and −12 ppm were previously assigned to the presence of Keggin anion [21,22], the lacunar ($[PW_{11}O_{39}]^{7-}$) and the dimeric $[P_2W_{21}O_{71}]^{6-}$ species [23], respectively, interacting with TiO_2. The two latter species should be formed by partial degradation of TPA. Regarding the ^{29}Si MAS-NMR measurements, bulk TSA showed a signal at −84.7 ppm due to presence of TSA Keggin anion ($[SiW_{12}O_{40}]^{4-}$) (Fig. 1b.2) and the TiO_2-TSA sample exhibited a signal at −85 ppm (Fig. 1b.1) ascribed to the Keggin anion interacting with the TiO_2 surface. It was also observed the presence of a broad peak between −100 and −120 ppm and centered at −110 ppm (Fig. 1b.2 and b.3), which could be assigned to silicate species or lacunary species (such as $[SiW_{11}O_{39}]^{8-}$) coming from partial degradation of TSA [24,25].

MAS-NMR for ^{1}H nuclei analysis of bulk hydrated TPA and TSA (Fig. 2) revealed the presence of two signals at 7.5 and 6.8 ppm for TPA and 7.8 and 6.9 ppm for TSA (Fig. 2a.3 and b.3), which could be related to interactions between water and Keggin anion protons by forming H_3O^+ species [20]. Pristine TiO_2 samples exhibited one intense and broad signal at 5.6 ppm and other small at 1.5 ppm (Fig. 2a.2 and b.2), both corresponding to bridging and terminal titanol groups (Ti—OH) respectively [26]. TiO_2/TPA sample (Fig. 2a.1) showed the bridging Ti-OH signal broader than in pristine TiO_2 and with a chemical shift at 5.5 ppm while the tiny signal corresponding to terminal Ti—OH groups was observed at 1.6 ppm. TiO_2/TSA samples (2b.1) showed more or less the same shapes and chemical shift for bridging and terminal Ti-OH groups (5.5 and 1.7 ppm respectively), however, it was revealed two new signals at ca. 3.5 and 1.1 ppm which could be related with the presence of silanol (Si—OH) groups in SiO_2 [26]. Moreover, a very small peak can also be observed on the left tail of the main component at 6.8 ppm i.e. very close the position of the ^{1}H peak of pure TSA.

Fig. 3 shows the spectra of the same compounds with a long (5 ms) echo delay which removes all fast relaxing components such as the strongly dipolar-coupled titanol groups while keeping the isolated or rapidly moving species. The above-mentioned tiny signal is then observed in both TiO_2/TPA and TiO_2/TSA samples at 6.8 ppm in agreement with the presence Keggin anions of TPA and TSA interacting with TiO_2 surface and hence confirming the presence of acid Brönsted sites on the surface.

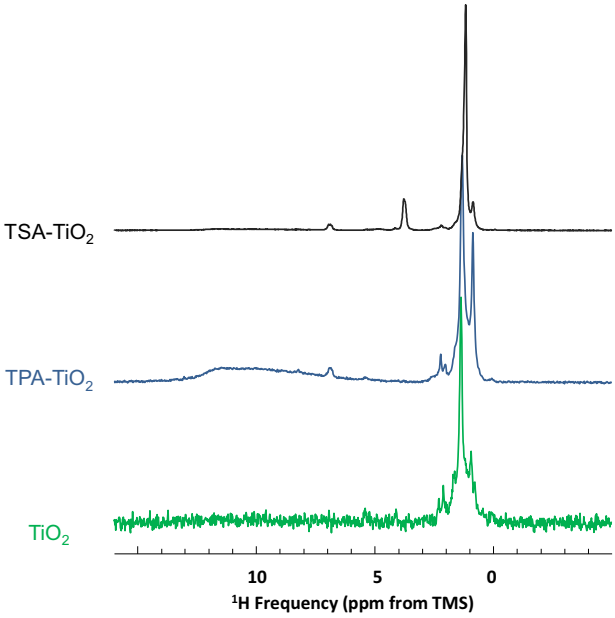

Fig. 3. ^{1}H MAS-NMR spectra obtained using a long delay (5 ms) Hahn echo aquisition selecting components with long (transverse) relaxation times.

It is also interesting to note the fact that for these surface species are shown in the same long delay echo acquisition means that they are very probably mobile, at least on the NMR time scale.

On the other hand, characterization by XRD (Fig. 4) revealed in all samples peaks corresponding to anatase TiO_2 at $2\theta = 25.3^\circ$, 37.9°, 47.8° and 54.3° [27]. XRD peaks related to TPA or TSA were not found, indicating that the heteropolyacids are highly dispersed on the titania matrix or as a noncrystalline phase. However, the TiO_2/TPA and TiO_2/TSA samples showed peak broadening and this fact is narrowly linked to the presence of the heteropolyacids, since previous studies have evidenced that the modification of TiO_2 with TPA or TSA retarded the crystallization of titania phase [21,28].

FT-Raman characterization showed the presence of anatase TiO_2 since it were found six Raman active modes ($A_{1g} + 2B_{1g} + 3E_g$), at 141.3 cm^{-1} (E_g), 197 cm^{-1} (E_g), 394.4 cm^{-1} (B_{1g}), 516.1 cm^{-1} (A_{1g}, B_{1g}), and 636.7 cm^{-1} (E_g) [29] (Fig. 5a). Bulk TPA showed intense Raman peaks typically assigned to the Keggin anion at 1080,

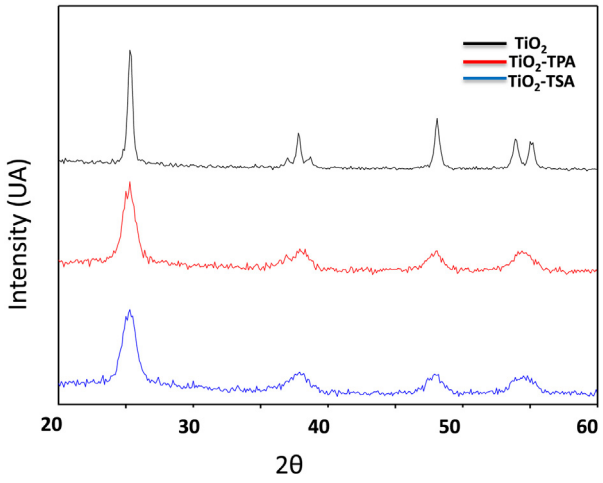

Fig. 4. XRD spectra of TiO_2, TiO_2-TPA and TiO_2-TSA samples.

990, 930, and 890 cm^{-1}, which are attributed to antisymmetric vibrations of P-O, W=O and W-O-W bonds [23] while bulk TSA exhibited FT-Raman peaks at 1000 cm^{-1}, 976 cm^{-1} and 926 cm^{-1} corresponding to ν_s (W-O), ν_{as} (W—O) and ν_{as} (W—O—W) respectively which agree very well with those of the Keggin anion of TSA [24,30].

The TiO_2/TPA and TiO_2/TSA samples showed two interesting Raman features. The first one was an important blue shifting of the most intense Raman peak of anatase TiO_2 at 141 cm^{-1} and attributed to Ti—O bonds (Fig. 5b). It was also found a strong peak

Table 1
Specific surface area, average pore dimeter (D_p) and acid strength (initial potential (E_i)).

Sample	BET specific surface area ($m^2\ g^{-1}$)	D_p (nm)[a]	E_i(mV)
TiO_2	57	4.1	150
TiO_2-TPA-30%	115	4.2	378
TiO_2-TSA-30%	126	4.3	398

[a] Average pore diameter calculated using the BJH formula from the desorption branch.

broadening in the TPA and TSA signals between 1080 and 900 cm^{-1} (Fig. 5c) which were assigned to W-O bonds. Both spectral changes could be due to strong interactions between TiO_2 and Keggin anions as has already described on the literature [27,31].

The N_2 adsorption–desorption isotherms of TiO_2, TiO_2/TPA and TiO_2/TSA samples (Fig. 6) can be classified as type IV, characteristic of mesoporous materials. The hysteresis loop was very small for TiO_2/TPA and TiO_2/TSA. These hysteresis loops (H2 type) are observed for solids made by aggregates of spheroidal particles with nonuniform size or shape pores [32].

The specific surface area (S_{BET}) of the samples determined from the N_2 adsorption–desorption isotherms using the Brunauer–Emmett–Teller (BET) method, together with the average pore diameter (*D*p), are shown in Table 1. As can be observed, all the samples present mainly mesopores with a *D*p in the range 4.1-4.3 nm. According with the pore size distribution of the samples (Fig. 6 inset), the addition of TPA and TSA produce wither mesoporos.

The pristine TiO_2 sample showed specific surface area lower (57 $m^2\ g^{-1}$) than the TiO_2/TPA (115 $m^2\ g^{-1}$) and TiO_2/TSA

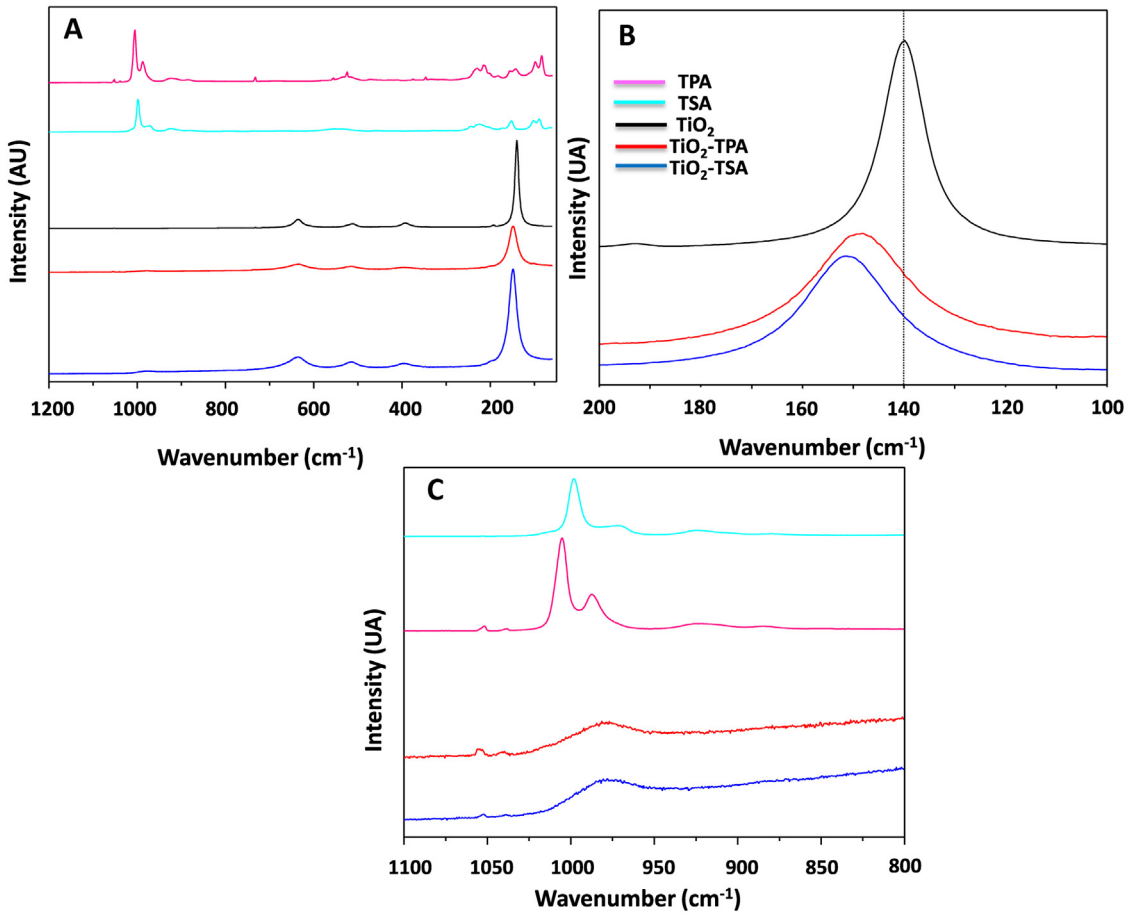

Fig. 5. FT-Raman spectra of TPA, TSA, TiO_2, TPA-TiO_2 and TSA-TiO_2 samples.

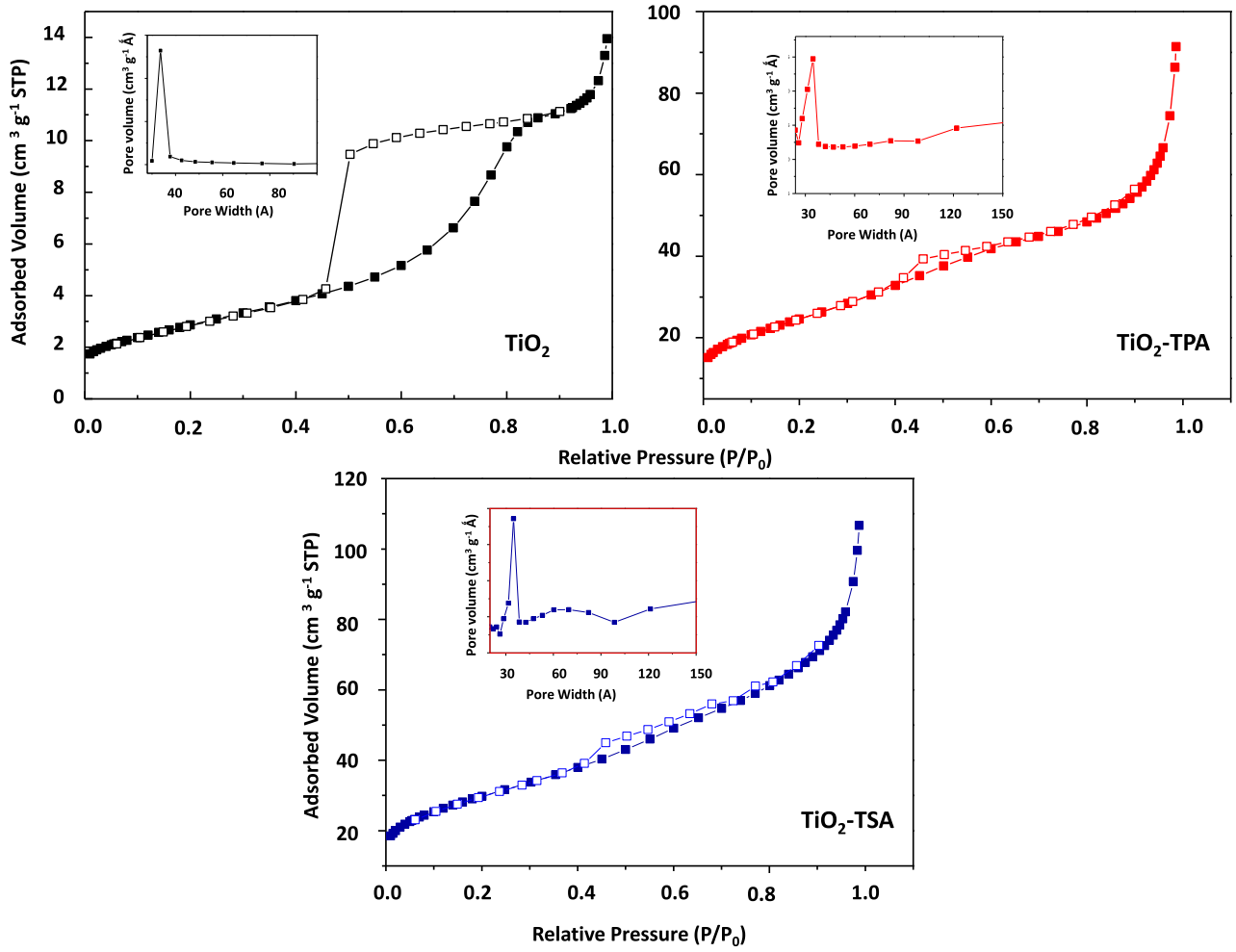

Fig. 6. N_2 adsorption–desorption isotherms of TiO_2, TiO_2-TPA and TiO_2-TSA samples.

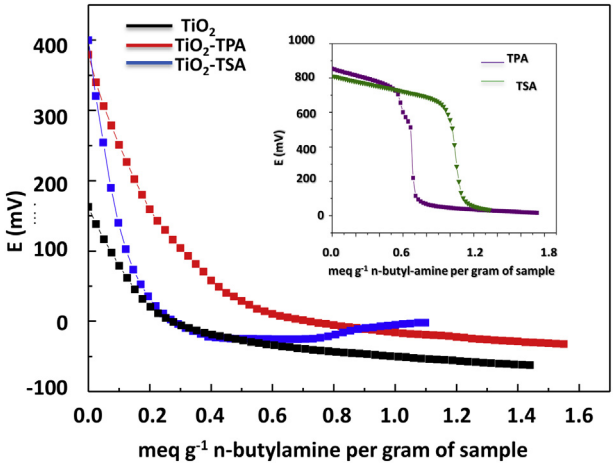

Fig. 7. Acid strength of TiO_2, TiO_2-TPA and TiO_2-TSA samples by potentiometric titration with *n*-butyl amine.

(126 $m^2\,g^{-1}$) samples. The higher S_{BET} values of TiO_2/TPA and TiO_2/TSA samples could be due to a strong interaction of the heteropolyacid (TPA or TSA) with the Ti—OH groups, which reduces the surface diffusion of titania, and inhibits sintering [21,28,33].

Since acidity is a key factor in esterification reactions, the acid strength was measured by potentiometric titration (Fig. 7). As a criterion to interpret the obtained results, it was suggested that the initial electrode potential (E_i) indicates the maximum acid strength of the sites and the value of meq amine g^{-1} solid where the plateau is reached indicates the total number of acid sites. The acid strength of these sites may be classified according to the scale reported in previous studies [34,35].

Bulk TPA and TSA have a very strong acidity since a high initial potential (800 and 850 mV respectively) was observed. In opposite, anatase TiO_2 revealed a lower strength acidity (E_i = 150 mV). TiO_2/TPA and TiO_2/TSA samples showed a high acid strength with E_i = 378 and 398 mV, respectively. These initial potentials were lower than those of bulk TPA and TSA but higher than pristine anatase TiO_2 sample. The lower acid strength of the TiO_2/TPA and TiO_2/TSA samples compared to bulk HPA could be assigned to the fact that the protons in the TPA and TSA are present as $H^+(H_2O)_n$ species whereas in the titania modified samples they are interacting with the oxygen of the Ti—OH groups.

It is well known that very acid protons of Keggin anion of TPA could easily interact with titanol (Ti—OH) surface groups of titania by protonating them and forming acid surface species such as ($\equiv TiOH_2^+$)($H_2PW_{12}O_{40}^-$) and ($\equiv TiOH_2^+$)$_2$($HPW_{12}O_{40}^{2-}$) [22,27]. However, not all TPA survives as Keggin anion since it was found evidence about partial degradation producing lacunar or dimeric species; this partial degradation could be due to the preparation method, where urea is used as forming pore agent producing ammonia (coming from urea hydrolysis) and slightly increasing pH solution or by thermal treatment [27,36]. Follow-

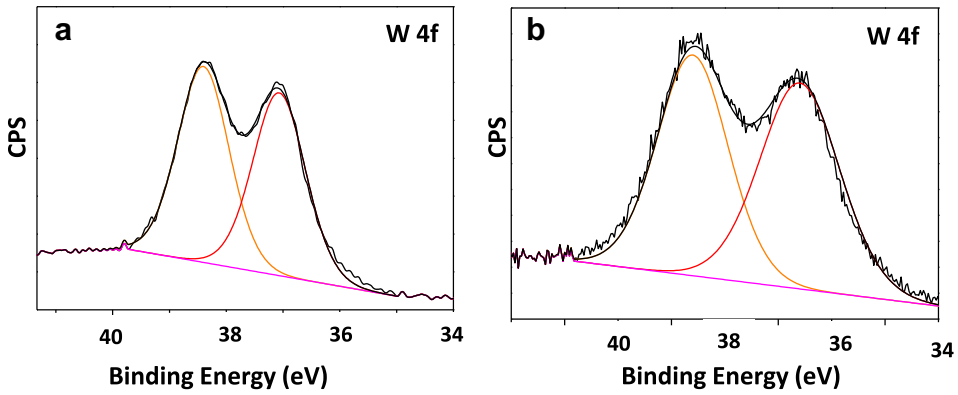

Fig. 8. W 4f XPS signal of (a) TiO_2-TPA and (b) TiO_2-TSA.

Table 2
Catalytic activity in conversion (%) of 2-furoic acid to 2-phenoxyethyl-2-furoate under different experimental conditions.

Entry	Catalyst Type	Temperature (°C)	Catalyst amount (mg)	Molar ratio acid/alcohol (mmol)	Conversion[a] (%)
1	–	125	–	1:10	15
2	TiO_2	125	50	1:10	17
3	TSA/TiO_2	125	50	1:10	57
4	TPA/TiO_2	125	50	1:10	76
5	TPA/TiO_2	125	50	1:5	77
6	TPA/TiO_2	125	50	1:2	91
7	TPA/TiO_2	110	50	1:2	77
8	TPA/TiO_2	95	50	1:2	21
9	TPA/TiO_2	140	50	1:2	95
10	TPA/TiO_2	125	25	1:2	80
11	TPA/TiO_2	125	100	1:2	90

[a] Conversion of 2-furoic acid to 2-phenoxyethyl-2-furoate measured after 7 h of catalytic reaction.

ing the previous statement and although TSA interactions with TiO_2 has not been well described in the literature, it is possible to suggest that acid protons of TSA could also interact with Ti-OH surface groups of the same way as TPA, forming surface acid species $(\equiv TiOH_2^+)_x(H_{4-x}SiW_{12}O_{40}^{x-})$ [27,37,38]. TSA underwent also partial degradation since a wide NMR ^{29}Si signal between −100 and −120 ppm was found. This signal could be due to the presence of amorphous silica Q_4 species or lacunar species such as $[SiW_{11}O_{39}]^{8-}$.

High resolution XPS spectra of W 4f for TiO_2/TPA and TiO_2/TSA samples (Fig. 8a and b respectively) revealed the presence of a doublet with binding energies at 38.2 and 36.2 eV corresponding to W (VI) which is often present in TPA and TSA [39,40]. Literature reports that Keggin anions of bulk TPA and TSA show also a doblet in the W 4f signal at BE of 37.9 and 35.8 eV respectively. There is a slight shifting between the signals reported for bulk TPA or TSA and those found in TiO_2/TPA and TiO_2/TSA samples. This shifting is too small for being attributed to a change in the oxidation state of W atoms, and should be related to some interaction between the Keggin anion and the TiO_2 surface. Furthermore, XPS results suggest that TPA and TSA Keggin anions should be present on the TiO_2 surface.

3.2. Catalytic tests: synthesis of 2-phenoxyethyl-2-furoate by esterification of 2-furoic acid and 2-phenoxyethanol

The synthesis of 2-phenoxyethyl-2-furoate by esterification of 1 mmol of 2-furoic acid with 10 mmol of 2-phenoxyethanol was evaluated using TiO_2/TPA and TiO_2/TSA samples as catalysts and catalyst absence (blank) under solvent free conditions and heating at 125 °C (Table 2). Apparition of 2-phenoxyethyl-2-furoate was followed by gas chromatography (GC) and these results showed that TiO_2/TPA sample exhibited the highest catalytic activity since a 2-furoic acid conversion of 77% was achieved after 7 h of reaction while TiO_2/TSA sample exhibited a conversion percentage of 57% (Table 2). The reaction in the absence of catalyst was also evaluated, obtaining just 15% of conversion in the same time. Although TiO_2/TSA sample presented a slight high acid strength and higher specific surface area than TiO_2/TPA, it is probable that this latter shows higher content of acid sites such as $(\equiv TiOH_2^+)(H_2PW_{12}O_{40}^-)$ and $(\equiv TiOH_2^+)_2(HPW_{12}O_{40}^{2-})$, this fact could explain its better catalytic performance in comparison with TiO_2/TSA sample.

Since the TiO_2/TPA sample showed the highest catalytic activity, it was proceed to evaluate this reaction upon different experimental conditions such as temperature, catalyst amount and molar 2-furoic acid to 2-phenoxyethanol ratio of in order to find the optimal reaction conditions.

When molar ratio acid:alcohol was 1:2 (Table 2), the catalytic reaction showed a higher performance (91% of conversion) than those obtained at molar ratios of 1:5 (77% of conversion) and 1:10 (76% of conversion). This was probably due to the fact that high alcohol content should act as a solvent, diluting the reagents and producing a detrimental effect on the contact between the acid and catalyst. In opposite, the molar ratio 1:2 might allow that the reaction be carried out upon solvent free conditions.

The effect of the reaction temperature was evaluated fixing the molar ratio at 1:2 (Table 2). At 95 °C, the catalytic performance was poor since the percentage of conversion was around 21% after 7 h under reaction. When temperature is risen to 110 °C, the conversion increased to c.a. 77%. Further temperature rising up to 125 °C, led to a conversion close to 91% after 7 h of reaction, however, when temperature reached 140 °C it was just observed an slight enhancement on the catalytic activity since the conversion was also around 95% after 7 h of reaction. Since esterification reactions are reversible and produce water as byproduct, at temperatures beyond 100 °C, water should be evaporated displacing the equilibria to the ester formation obtaining a high conversion.

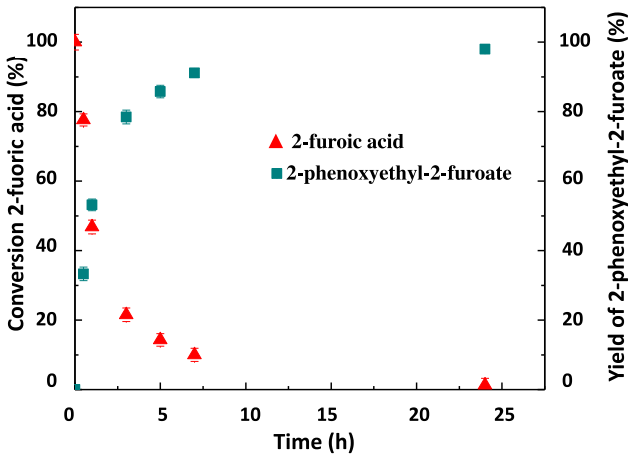

Fig. 9. 2-fuoric acid disappearance and 2-phenoxyethyl-2-furoate formation under catalytic test at the best conditions.

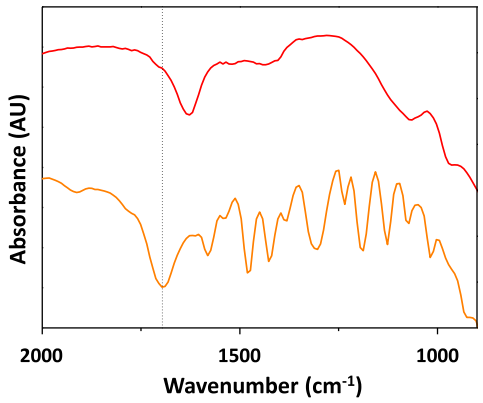

Fig. 10. DRIFT-FT-IR spectra of 2-furoic acid (orange) and 2-fuoric acid adsorbed on TiO_2-TPA sample (red). (For interpretation of the references to colour in this figure legend, the reader is referred to the web version of this article.)

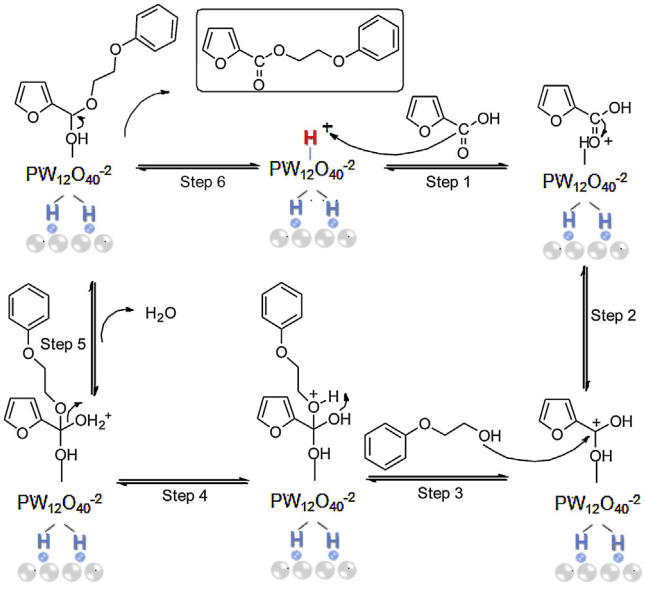

Fig. 11. Suggested mechanism of esterification reaction of 2-furoic acid with 2-phenoxyethanol.

It was also studied the effect of the catalyst amount on the reaction, fixing the reagents molar ratio at 1:2 and temperature at 125 °C (Table 2). When catalyst amounts of 25, 50 and 100 mg were used, the percentage of 2-furoic acid conversion was 80, 91 and 90%, respectively after 7 h of catalytic reaction. This suggests that catalyst amount (at least the amounts used in this study) was not a critical issue in the synthesis of 2-phenoxyethyl-2-furoate and the amount of 50 mg was chosen as the best.

Finally, and in order to observe simultaneously the disappearance of 2-furoic acid and the formation of 2-phenoxyethyl-2-furoate, GC experiments were carried out measuring both compounds (Fig. 9). It was clear that 2-fuoric acid disappears at the same time that 2-phenoxyethyl-2-furoate starts its formation, and other byproducts were not observed. Characterization by ^{1}H and ^{13}C NMR and mass spectrometry confirmed the presence of 2-phenoxyethyl-2-furoate (section 2.5).

The 2-furoic conversion at different catalyst reusing cycles using the optimal conditions of molar ratio, temperature and TiO_2/TPA were measured. The results obtained show that in the first reusing cycle conversion decreased from 98 to 92%, which may be due either to a loss of catalytic activity caused by poisoning of the catalyst active sites or to TPA leaching. The latter could be the most probable cause since when a control experiment was performed using the reagents (2-furoic acid and 2-phenoxyetanol) obtained after the filtration of the catalyst, the conversion was slightly superior to the control experiment performed in absence of catalyst (19% vs 11% after 7 h of reaction). This catalytic activity rising should be related to the presence of leached TPA leading to a homogeneous catalytic esterification reaction. The two last reusing cycles did not undergo a remarkable loss of catalytic activity (85 and 84%, respectively). This could be due to the weakly anchored TPA molecules were leached in the first two cycles remaining only on the solid those heteropolyacid molecules which are strongly anchored.

It was studied by DRIFT FT-IR spectroscopy, the interaction between 2-fuoric acid and TPA-TiO_2 sample (Fig. 10). After 24 h of contact between the acid and the TiO_2/TPA sample, it was observed that the typical C=O signal characteristic of organic acids at 1700 cm^{-1} underwent a shifting towards 1650 cm^{-1}, indicating that 2-furoic acid could be strongly interacting with TiO_2/TPA sample surface. This agree well with the proposed mechanisms of esterification with acid solid catalysts, where the acid interacts with Brönsted acid sites, in this case $(\equiv TiOH_2^+)(H_2PW_{12}O_{40}^-)$ and $(\equiv TiOH_2^+)_2(HPW_{12}O_{40}^{2-})$ present on the TiO_2/TPA sample. These acid sites can lead the formation of protonated 2-fuoric acid species polarizing the C=O bond which may easily react with the alcohol producing the corresponding ester and water (Fig. 11).

4. Conclusions

Tungstophosphoric (TPA) and tungstosilicic (TSA) acid were successfully immobilized on TiO_2 supports (TiO_2/TPA and TiO_2/TSA samples). The characterization revealed that the most part of the heteropolyacids, either TSA or TPA could be present on the support as Keggin anions exhibiting very acid sites such as $(\equiv TiOH_2^+)(H_2PW_{12}O_{40}^-)$ and $(\equiv TiOH_2^+)_2(HPW_{12}O_{40}^{2-})$ for TiO_2-TPA and $(\equiv TiOH_2^+)_x(H_{4-x}SiW_{12}O_{40}^{-x})$ for TiO_2-TSA.

The obtained conversion, which was evaluated in the esterification of 2-furoic acid with 2-phenoxyethanol to lead the formation of 2-phenoxyethyl-2-furoate showed that the TiO_2/TPA sample led to the highest catalytic activity probably due to the presence of acid sites on the solid. The catalyst amount, temperature and molar ratio acid:alcohol were evaluated as variables. The last two, temperature and acid:alcohol molar ratio, were the most important variables. Temperatures beyond to 100 °C allow evaporating the water, displacing the equilibria to the ester formation and obtaining a high catalytic activity. On the other hand, an acid:alcohol molar

ratio with low alcohol content (1:2) was found as optimal since at high alcohol content, this latter should act as a solvent, diluting the reagents and producing a detrimental effect in the contact between the acid and catalyst. At low alcohol contents, the reaction could be carried out upon solvent free conditions.

Finally, DRIFT-FT-IR measurements gave evidence about that a strong 2-fuoric acid interaction with the acid sites of the TiO_2/TPA sample, such as ($\equiv TiOH_2^+$)($H_2PW_{12}O_{40}^-$) and ($\equiv TiOH_2^+$)$_2$($HPW_{12}O_{40}^{2-}$), should be an important step reaction since it should polarize the C=O bond, allowing the 2-phenoxyethanol attack and achieving the esterification reaction.

Acknowledgements

Authors thank the financial support from CONICET and Universidad Nacional de La Plata (UNLP) and the technical assistance of Liliana Bertini (CIMA-ITBA) and Lilian Osiglio in the DRIFT-FTIR and potentiometric analysis respectively.

Referencias

[1] E. Papaconstantinau, Photochemistry of polyoxometallates of molybdenum, and tungsten and/or vanadium, Chem. Soc. Rev. 18 (1989) 1–31.
[2] I.V. Kozhevnikov, Catalysis by heteropoly acids and multicomponent polyoxometallates in liquid-phase reactions, Chem. Rev. 98 (1998) 171–198.
[3] J.G. Hernández-Cortéz, M.A. Manríquez, L. Lartundo-Rojas, E. López-Salinas, Study of acid-base properties of supported heteropoly acids in the reactions of secondary alcohols dehydration, Catal. Today 220–222 (2014) 32–38.
[4] M.E. Pérez, D.M. Ruiz, J.C. Autino, M.N. Blanco, L.R. Pizzio, G.P. Romanelli, Mesoporous titania/tungstophosphoric acid composites: suitable synthesis of flavones, J. Porous Mater. 20 (2013) 1433–1440.
[5] A. Popa, V. Sasca, I. Holclajtner-Antunovic, The influence of surface coverage on textural, structural and catalytic properties of cesium salts of 12-molybdophosphoric acid supported on SBA-15 mesoporous silica, Microporous Mesoporous Mater. 156 (2012) 127–137.
[6] L.R. Pizzio, P.G. Vázquez, C.V. Cáceres, M.N. Blanco, Supported Keggin type heteropolycompounds for ecofriendly reactions, Appl. Catal. A: Gen. 256 (2003) 125–139.
[7] M.N. Blanco, L.R. Pizzio, Properties of mesoporous tungstosilicic/titania composites prepared by sol-gel method, Appl. Surf. Sci. 256 (2010) 3546–3553.
[8] T.S. Rivera, A. Sosa, G.P. Romanelli, M.N. Blanco, L.R. Pizzio, Tungstophosphoric acid/zirconia composites prepared by the sol-gel method: an efficient and recyclable green catalyst for the one-pot synthesis of 14-aryl-14H-dibenzo[a,j]xanthenes, Appl. Catal. A: Gen. 443–444 (2012) 207–213.
[9] A. Corma, S. Iborra, A. Velty, Chemical routes for the transformation of biomass into chemicals, Chem. Rev. 107 (2007) 2411–2502.
[10] A.K. Chakraborti, B. Singh, S.V. Chankeshwara, A.R. Patel, Protic acid immobilized on solid support as an extremely efficient recyclable catalyst system for a direct and atom economical esterification of carboxylic acids with alcohols, J. Org. Chem. 74 (2009) 5967–5974.
[11] K. Tanaka, F. Toda, Solvent-free organic synthesis, Chem. Rev. 100 (2000) 1025–1074.
[12] J. Otera, Esterification Methods Reactions and Applications, Wiley-VCH, Weinheim, 2003.
[13] M.R. Altiokka, E. Akbay, Z. Him, Impregnation of 12-tungstophosphoric acid on tonsil: an effective catalyst for esterification of formic acid with n-butyl alcohol and kinetic model, J. Mol. Catal. A: Chem. 385 (2014) 18–25.
[14] A. Patel, V. Brahmkhatri, Kinetic study of oleic acid esterification over 12-tungstophosphoric acid catalyst anchored to different mesoporous silica supports, Fuel Process. Technol. 113 (2013) 141–149.
[15] C.O. Tuck, E. Pérez, I.T. Horváth, R.A. Sheldon, M. Poliakoff, Valorization of biomass: deriving more value from waste, Science 337 (2012) 695–699.
[16] F.W. Lichtenthaler, S. Peters, Carbohydrates as green raw materials for the chemical industry, C.R. Chim. 7 (2004) 65–90.
[17] A. Escobar, A. Sathicq, L. Pizzio, M. Blanco, G. Romanelli, Biomass valorization derivatives: clean esterification of 2-furoic acid using tungstophosphoric acid/zirconia composites as recyclable catalyst, Process Saf. Environ. 98 (2015) 176–186.
[18] J.A. Rengifo-Herrera, M. Blanco, J. Wist, P. Florian, L.R. Pizzio, TiO_2 modified with polyoxotungstates should induce visible-light absorption and high photocatalytic activity through the formation of surface complexes, Appl. Catal. B: Environ. 189 (2016) 99–109.
[19] F. Lefebvre, ^{31}P MAS NMR study of $H_3PW_{12}O_{40}$ supported on silica: formation of ($\equiv SiOH_2$ +)($H_2PW_{12}O_{40}^-$), J. Chem. Soc. Chem. Commun. 10 (1992) 756–757.
[20] N. Essayem, Y.Y. Tong, H. Jobic, J.C. Vedrine, Characterization of protonic sites in $H_3PW_{12}O_{40}$ and $Cs_{1.9}H_{1.1}PW_{12}O_{40}$: a solid-state ^{1}H ^{2}H, ^{31}P MAS-NMR and inelastic neutron scattering study on samples prepared under standard reaction conditions, Appl. Catal. A: Gen. 194–195 (2000) 109–122.
[21] V.M. Fuchs, E.L. Soto, M.N. Blanco, L.R. Pizzio, Direct modification with tungstophosphoric acid of mesoporous titania synthesized by urea-templated sol-gel reactions, J. Colloid Interface Sci. 327 (2008) 403–411.
[22] J.C. Edwards, C.Y. Thiel, B. Benac, J.F. Knifton, N.M.R. Solid-state and, FT-IR investigation of 12-tungstophosphoric acid on TiO_2, Catal. Lett. 51 (1998) 77–83.
[23] I. Holclajtner-Antunovic, D. Bajuk-Bogdanovic, A. Popa, S. Uskokovic-Markovic, Spectroscopic identification of molecular species of 12-tungstophosphoric acid in methanol/water solutions, Inorg. Chim. Acta 383 (2012) 26–32.
[24] D.P. Sawant, A. Vinu, S.P. Mirajkar, F. Lefebvre, K. Ariga, S. Anandan, T. Mori, C. Nishimura, S.B. Halligudi, Silicotungstic acid/zirconia immobilized on SBA-15 for esterifications, J. Mol. Catal. A: Chem. 271 (2007) 46–56.
[25] V. Brahmkhatri, A. Patel, Synthesis and characterization of 12-tungstosilicic acid anchored to MCM-41 as well as its use as environmentally benign catalyst for synthesis of succinate and malonate diesters, Ind. Eng. Chem. Res. 50 (2011) 13693–13702.
[26] M. Crocker, A.M. Herold, A.E. Wilson, M. Mackay, C.A. Emeis, A.M. Hoogendoorn, ^{1}H NMR spectroscopy of titania: chemical shift assignments for hydroxy groups in crystalline and amorphous forms of TiO_2, J. Chem. Soc. Faraday Trans. 92 (1996) 2791–2798.
[27] S. Gelover, P. Mondragon, A. Jimenez, Titanium dioxide sol-gel deposited over glass and its application as a photocatalyst for water decontamination, J. Photochem. Photobiol. A 165 (2004) 241–246.
[28] S.M. Kumbar, G.V. Shanbhag, F. Lefebvre, S.B. Halligudi, Heteropoly acid supported on titania as solid acid catalyst in alkylation of p-cresol with tert-butanol, J. Mol. Catal. A: Chem. 256 (2006) 324–334.
[29] A. Li Bassi, D. Cattaneo, V. Russo, C.E. Bottani, E. Barborini, T. Mazza, P. Piseri, P. Milani, F.O. Ernst, K. Wegner, S.E. Pratsinis, Raman spectroscopy characterization of titania nanoparticles produced by flame pyrolysis: the influence of size and stoichiometry, J. Appl. Phys. 98 (2005) 074305-1–074305-9.
[30] M.B. Colovic, D. Bajuk-Bogdanovic, N.S. Avramovic, I. Holclajtner-Antunovic, N.S. Bosnjakovic-Pavlovic, V.M. Vasic, D.Z. Krstic, Inhibition of rat synaptic membrane Na^+/K^+-ATPase and ecto-nucleoside triphosphate diphosphohydrolases by 12-tungstosilicic and 12-tungstophosphoric acid, Bioorgan. Med. Chem. 19 (2011) 7063–7069.
[31] J. Li, W. Kang, X. Yang, X. Yu, L. Xu, Y. Guo, H. Fang, S. Zhang, Mesoporous titania-based $H_3PW_{12}O_{40}$ composite by a block copolymer surfactant-assisted templating route: preparation, characterization, and heterogeneous photocatalytic properties, Desalination 255 (2010) 107–116.
[32] G. Leofanti, M. Padovan, G. Tozzola, B. Venturelli, Surface area and pore texture of catalysts, Catal. Today 41 (1998) 207–219.
[33] X.-F. Yu, N.-Z. Wu, H.-Z. Huang, Y.-C. Xie, Y.-Q. Tang, A study on the monolayer dispersion of tungsten oxide on anatase, J. Mater. Chem. 11 (2001) 3337–3342.
[34] D.O. Bennardi, G.P. Romanelli, J.C. Autino, L.R. Pizzio, Supported trifluoromethanesulfonic acid as catalyst in the synthesis of flavone and chromone derivatives, Appl. Catal. 324 (2007) 62–68.
[35] L.R. Pizzio, M.N. Blanco, Isoamyl acetate production catalyzed by $H_3PW_{12}O_{40}$ on their partially substituted Cs or K salts, Appl. Catal. A: Gen. 255 (2003) 265–277.
[36] J.A. Rengifo-Herrera, M.N. Blanco, L.R. Pizzio, Photocatalytic bleaching of aqueous malachite green solutions by UV-A and blue-light-illuminated TiO_2 spherical nanoparticles modified with tungstophosphoric acid, Appl. Catal. B: Environ. 110 (2011) 126–132.
[37] Y. Guo, Y. Yang, C. Hu, C. Guo, E. Wang, S. Feng, Preparation, characterization and photochemical properties of ordered macroporous hybrid silica materials based on monovacant Keggin-type polyoxometalates, J. Mater. Chem. 12 (2002) 3046–3052.
[38] Y. Guo, C. Hu, Porous hybrid photocatalysts based on polyoxometallates, J. Clust. Sci. 14 (2003) 505–526.
[39] P.A. Jalil, M. Faiz, M. Tabet, N.M. Hamdan, Z. Hussain, A study of the stability of tungstophosphoric acid $H_3PW_{12}O_{40}$, using synchrotron XPS, XANES, hexane cracking, XRD, and IR spectroscopy, J. Catal. 217 (2003) 292–297.
[40] R. Dziembaj, A. Malecka, Z. Piwowarska, A. Bielanski, XPS study of polyaniline supported dodecatungstosilicic acid catalyst, J. Mol. Catal. A: Chem. 12 (1996) 423–430.